



## RESEARCH ARTICLE



WILEY

# Intraspecific variability in human maxillary bone modeling patterns during ontogeny

Alexandra Schuh<sup>1</sup> | Philipp Gunz<sup>1</sup> | Chiara Villa<sup>2</sup> | Kornelius Kupczik<sup>1,3</sup> | Jean-Jacques Hublin<sup>1</sup> | Sarah E. Freidline<sup>1</sup>

<sup>1</sup>Department of Human Evolution, Max Planck Institute for Evolutionary Anthropology, Leipzig, Germany

<sup>2</sup>Laboratory of Advanced Imaging and 3D modelling, Section of Forensic Pathology, Department of Forensic Medicine, University of Copenhagen, Copenhagen, Denmark

<sup>3</sup>Max Planck Weizmann Center for Integrative Archaeology and Anthropology, Max Planck Institute for Evolutionary Anthropology, Leipzig, Germany

**Correspondence**

Alexandra Schuh, Department of Human Evolution, Max Planck Institute for Evolutionary Anthropology, Deutscher Platz 6, 04103, Leipzig, Germany.  
Email: alexandra\_schuh@eva.mpg.de

**Abstract**

**Objectives:** This study compares the ontogenetic bone modeling patterns of the maxilla to the related morphological changes in three human populations to better understand how morphological variability within a species is established during ontogeny at both micro- and macroscopic levels.

**Materials and methods:** The maxillary bones of an ontogenetic sample of 145 subadult and adult individuals from Greenland (Inuit), Western Europe (France, Germany, and Portugal), and South Africa (Khoekhoe and San) were analyzed. Bone formation and resorption were quantified using histological methods to visualize the bone modeling patterns. In parallel, semilandmark geometric morphometric techniques were used on 3D models of the same individuals to capture the morphological changes. Multivariate statistics were applied and shape differences between age groups were visualized through heat maps.

**Results:** The three populations show differences in the degree of shape change acquired during ontogeny, leading to divergences in the developmental trajectories. Only subtle population differences in the bone modeling patterns were found, which were maintained throughout ontogeny. Bone resorption in adults mirrors the pattern found in subadults, but is expressed at lower intensities.

**Discussion:** Our data demonstrate that maxillary morphological differences observed in three geographically distinct human populations are also reflected at the microscopic scale. However, we suggest that these differences are mostly driven by changes in rates and timings of the cellular activities, as only slight discrepancies in the location of bone resorption could be observed. The shared general bone modeling pattern is likely characteristic of all *Homo sapiens*, and can be observed throughout ontogeny.

**KEYWORDS**

bone formation, bone resorption, facial ontogeny, semilandmark geometric morphometrics

## 1 | INTRODUCTION

Among present day humans, geographic variation in adult facial morphology has been reported as reflecting population affinities

(Hanihara, 1996, 2000; Hennessy & Stringer, 2002; Howells, 1973, 1989; Lynch, Wood, & Luboga, 1996). In addition to population history, environmental factors such as climate and subsistence strategies contribute to cranial shape variation among human populations.

This is an open access article under the terms of the Creative Commons Attribution License, which permits use, distribution and reproduction in any medium, provided the original work is properly cited.

© 2020 The Authors. *American Journal of Physical Anthropology* published by Wiley Periodicals LLC.

Adaptation to climate has been observed in facial features (Butaric & Maddux, 2016; Cui & Leclercq, 2017; Evteev, Cardini, Morozova, & O'Higgins, 2013; Harvati & Weaver, 2006; Hubbe, Hanihara, & Harvati, 2009; Nicholson & Harvati, 2006; Roseman & Weaver, 2004), particularly in the shape of the nasal region (Churchill, Shackelford, Georgi, & Black, 2004; Franciscus & Long, 1991; Holton & Franciscus, 2008; Maddux, Yokley, Svoma, & Franciscus, 2016; Yokley, 2009). Noback, Harvati, and Spoor (2011), as well as Maddux, Butaric, Yokley, and Franciscus (2017), found correlations between cold-dry and hot-wet environments and the shape of the bony nose (particularly the nasal fossa), suggesting that aspects of the nasorespiratory system may be adaptations to particular environments. Moreover, according to several studies changes in diet across time as observed between hunter-gatherer and agricultural populations have been linked to the gracilization of the masticatory apparatus (Deter, 2009; Gonzalez-Jose et al., 2005; Noback & Harvati, 2015; Stynder, Ackermann, & Sealy, 2007; von Cramon-Taubadel, 2011). Stansfield, Evteev, and O'Higgins (2018) suggested that a reduction of loadings during ontogeny explains morphological differences in the mandible between prehistoric and modern humans. Thus, in comparison to the rest of the skull, facial components may be more plastic being subjected to diverse sources of variation (Smith, 2009; von Cramon-Taubadel, 2014).

One way to understand how morphological variability is established within a species is by investigating its ontogenetic processes. Freidline, Gunz, and Hublin (2015) compared the ontogenetic and static allometry (i.e., the covariation between shape and size) of several geographically diverse human populations using geometric morphometric techniques. Their results support previous studies by showing that population differences in facial morphology are already present early in ontogeny, possibly prenatally (e.g., Bastir & Rosas, 2004; Lieberman, McBratney, & Krovitz, 2002; Mooney & Siegel, 1986; Nicholas, 2016; Ponce de Leon & Zollikofer, 2001). They also demonstrated subtle differences between populations in the patterns of absolute and relative growth and development. Therefore, changes in the patterns of ontogenetic allometry generate differences in facial morphology between human populations (Bulygina, Mitteroecker, & Aiello, 2006; Rosas & Bastir, 2002; Sardi & Ramirez-Rozzi, 2012; Vidarsdóttir, O'Higgins, & Stringer, 2002).

At the cellular level, both the rate of activity as well as the location on bone surfaces of the osteoblasts and osteoclasts, the cells responsible for bone formation (or apposition; Enlow & Bang, 1965, Enlow, 1966) and resorption, cause bone to change in size and shape during ontogeny. This process, visible on dry bone, is called bone modeling (Enlow, 1962; Enlow & Bang, 1965; Frost, 1987). It is of particular interest for ontogenetic studies as it can help us better understand the development of morphological features (Bromage, 1989; McCollum, 1999; McCollum, 2008). A majority of the ontogenetic studies published in the past 20 years employed geometric morphometric techniques as a methodological approach, as it is a powerful tool for the quantification and visualization of morphological changes (Gunz & Mitteroecker, 2013; Mitteroecker & Gunz, 2009; Mitteroecker, Gunz, Windhager, & Schaefer, 2013). However, few studies have focused on the relationship between bone modeling

patterns and morphological changes during ontogeny. This was first assessed by O'Higgins and Jones (1998) in the Red-capped mangabey *Cercocebus torquatus*. The authors found that the bone modeling patterns reflect allometric patterns in the face of this species. Several recent studies combined surface histology and semilandmark geometric morphometric techniques to study facial ontogeny in great apes and humans (Freidline, Martinez-Maza, Gunz, & Hublin, 2016; Martinez-Maza, Freidline, Strauss, & Nieto-Diaz, 2015; Schuh, Kupczik, Gunz, Hublin, & Freidline, 2019). Such as O'Higgins and Jones (1998), these studies showed a correspondence between the morphological changes and the bone modeling patterns. Furthermore, these methods have shown to be complementary: while surface histology is informative about the microscopic processes underlying bone growth, geometric morphometric techniques help to quantify and visualize the morphological changes and displacements that cannot be observed through bone modeling alone.

Recently, Schuh et al. (2019) applied both methods on an ontogenetic sample of 48 maxillae from French individuals. In line with previous studies (Martinez-Maza et al., 2015; O'Higgins & Jones, 1998), the authors observed that maxillary bone modeling patterns in humans are rather constant through time from early stages on (i.e., the location of bone resorption on the surface is similar between age groups). This implies that the resorptive process is highly controlled (as discussed by Schulte et al., 2013), and that morphological differences within a group are likely driven by changes in bone formation and resorption rates rather than major differences in the bone modeling patterns. Regions of the maxilla showing less morphological variation, such as the maxillary arcade, are associated mainly to resorptive areas, suggesting that regions of high mechanical demands are more constrained and less variable. However, these inferences are based on a single population and may not reflect the variability within a species. McCollum (2008) proposed that the differences in the expression of bone resorption observed in her sample may reflect population history; however, like most bone modeling studies the limited sample size, as well as the lack of quantitative data, make this interpretation difficult.

In the present study, we quantify the bone modeling patterns in an ontogenetic series of three geographically distinct human populations: Western European, Greenlandic Inuit, and South African Khoekhoe and San descent. We investigate if differences observed at the macroscopic (or morphological) scale relate to those at the microscopic level. The Inuit facial morphology has long been the focus of many studies (Cruwys, 1988; Hawkes, 1916; Hrdlička, 1910; Hylander, 1977; Lynnerup, Homøe, & Skovgaard, 1999; Oschinsky, 1962), and different hypotheses have been proposed to explain their characteristic facial features, such as adaptation to a cold environment (Coon, Garn, & Birdsell, 1950; Wolpoff, 1968) and a hard diet (Hrdlička, 1910; Hylander, 1977). They are characterized by an elongated, narrow nasal aperture, vertical zygomatic processes, reduced nasal bones, and maxillary frontal process width, as well as a generally flat infra orbital area (Hylander, 1977). South African populations such as Khoekhoe and San possess small faces with short and wide nasal apertures, anteriorly projecting zygomatic processes, wide orbits, and large maxillary frontal processes (Freidline et al., 2015). Europeans have been described as

showing long noses and retracted zygomatic bones (Hennessy & Stringer, 2002). Thus, we expect discrepancies in the expression and/or location of bone resorption between these populations where shape differences are the most pronounced, for example in the nasal area for which population differences have been described (Hennessy & Stringer, 2002; Maddux et al., 2017; Noback et al., 2011; Sardi & Ramirez-Rozzi, 2012). Moreover, a more pronounced canine fossa should be associated with more bone resorption, as discussed by Enlow and Bang (1965) and Schuh et al. (2019).

## 2 | MATERIALS AND METHODS

### 2.1 | Sample

The cross-sectional ontogenetic sample comprises 145 individuals from three different geographic areas (refer to Table 1 for the sample composition): Western Europe (Anatomical Institute of Strasbourg, France; Anatomical Institute of the University of Leipzig, Germany; Anthropological collection of the University of Coimbra, Portugal), Greenland (Inuit; Laboratory of Biological Anthropology, University of Copenhagen, Denmark) and South Africa (Khoekhoe and San; Iziko South African Museum, Cape Town; Anthropological collection of the Department of Human Biology, University of Cape Town; McGregor Museum, Kimberley, South Africa). Sex and calendar ages are known for some Western European individuals only, and were already previously investigated (Schuh et al., 2019). Thus, they were not considered in this study. We divided our sample into four age groups based on dental development, following AlQahtani, Hector, and Liversidge (2010): AG 1, developing deciduous dentition; AG 2, first permanent molar (M1) in occlusion; AG 3, second permanent molar (M2) in occlusion; AG 4, third permanent molar (M3) erupted, or adults. For the latter, variability in the bone modeling patterns is still largely unknown; however, as adult maxillae are larger than those of subadults, data collection is more time-consuming. Therefore, we were only able to include a limited number of individuals for this group. Finally, individuals with extensive tooth loss or surface alterations were avoided.

Negative molds of the maxillary surface (delimited by the surrounding sutures) were made using a low-viscosity silicone (President Plus light body, Coltène/Whaledent AG, Switzerland) following

Bromage (1989). A positive replica of each negative mold was generated using an epoxy resin (5 Minute Epoxy Epoxidharz 2 K-Kleber transparent, Devcon). Only the better-preserved side of the maxilla was kept for the analysis (i.e., either left or right). Out of the 145 individuals, seven did not yield any data, which reduced the sample size

**TABLE 2** Landmarks and semilandmarks numbers and definition (total: 249)

Landmarks	Label	
<b>Fixed landmarks</b>		
Superolateral nasion	sln	
Dacryon	d	
Zygoorbitale	zyo	
Inferolateral rhinion	ilr	
Anterior nasal spine	ans	
Alveolare (infradentale superius)	ids	
Zygomaxillare	zm	
Malar root origin	mro	
Maxillo-palatine suture	mps	
<b>Curve semilandmarks</b>		<b>Number—definition</b>
Fronto-maxillary suture	FMS	2—Superolateral nasion to dacryon
Naso-maxillary suture	NMS	6—Superolateral nasion to inferolateral rhinion
Inferior orbital margin	IOM	6—Dacryon to zygoorbitale
Nasal aperture outline	NA	6—Inferolateral rhinion to anterior nasal spine
Subnasal outline	SO	3—Nasal spine to alveolar
Zygomatiko-maxillary suture	ZMS	5—Zygoorbitale to zygomaxillare
Maxillary contour	MC	4—Zygomaxillare to malar root origin
Alveolar outline	AO	8—Alveolare to maxillo-palatine suture
<b>Surface semilandmarks</b>		200—Covering the whole surface of the bone

**TABLE 1** Number of individuals for each population and age group

Age group	Greenlandic Inuit <sup>a</sup>	South African <sup>b</sup>	Western European <sup>c</sup>	Total
1	13	11	24	48
2	15	8	27	50
3	15	8	3	19
4	5	10	6	21
<b>Total</b>	<b>48</b>	<b>37</b>	<b>60</b>	<b>145</b>

<sup>a</sup>Laboratory of Biological Anthropology, University of Copenhagen, Denmark.

<sup>b</sup>Iziko Museum of Cape Town; University of Cape Town; McGregor Museum of Kimberley, South Africa.

<sup>c</sup>Strasbourg Anatomical Collection (Le Minor, Billmann, Sick, Vetter, & Ludes, 2009; Rampont, 1994), France; Leipzig University of medicine, Germany; Anthropological Collection of the University of Coimbra, Portugal.

to 138 individuals for the surface histology analysis. Those individuals were however kept for the morphological analysis. We used computed tomography (CT) scans of all individuals acquired at a resolution of 0.2 to 0.4 mm (BIR ACTIS 225/300) and 0.6 mm for the Western European/South African individuals and Greenlandic Inuit, respectively. For the South African sample, some of the scans were acquired using a portable Artec Space Spider (Artec3D, Luxembourg) surface scanner. The surface models were generated using the software packages Avizo (Thermo Fisher Scientific) and Artec Studio.

## 2.2 | Analyses

### 2.2.1 | Analysis of developmental changes

To quantify the morphological changes of the maxilla bone during ontogeny, we used a template of 249 landmarks and semilandmarks (Table 2) created in Viewbox (dHAL software) from the right maxilla (Figure 1a). Fixed landmarks ( $n = 9$ ) and curve semilandmarks ( $n = 40$ ) were placed manually, and surface semilandmarks ( $n = 200$ ) were automatically projected onto each individual's surface using a thin-plate spline (TPS) interpolation function. Estimation of missing data was performed in RStudio (RStudio Team, 2020) by deforming the weighted estimate configurations that are the most similar to the defective configuration using a TPS interpolation (package Morpho;

Schlager, 2017). Landmarks taken on left maxillae were mirrored to obtain a sample composed of only right configurations. To assure geometric homology between the landmark configurations, the curve and surface semilandmarks were allowed to slide along their respective tangent axis and plane, by minimizing the bending energy of the deformation between the sample mean and each configuration (Bookstein, 1997; Gunz, Mitteroecker, & Bookstein, 2005).

The coordinates were then superimposed using a Generalized Procrustes Analysis (GPA; Rohlf & Slice, 1990). To first investigate the morphological variation in the ontogenetic patterns, developmental trajectories between populations were explored by using a Principal Component Analysis (PCA) in shape space. Shape differences between populations were visualized by computing and superimposing the mean shapes of each population. Differences and/or similarities in the developmental trajectories were assessed with the use of developmental simulations. In a given population, the youngest individuals (from AG 1) were simulated along the trajectory of another population by adding the mean developmental trajectory of the latter (computed as the vectors of the mean shape differences) to their Procrustes coordinates (Gunz, Neubauer, Maureille, & Hublin, 2010; Neubauer, Gunz, & Hublin, 2010; Scott, Neubauer, Hublin, & Gunz, 2014). As developmental trajectories are nonlinear, and as the number of variables largely exceeds the number of individuals in this study, performing linear statistical tests is not appropriate. By accounting for the nonlinearity of the trajectories, this method thus allows the analysis of ontogenetic

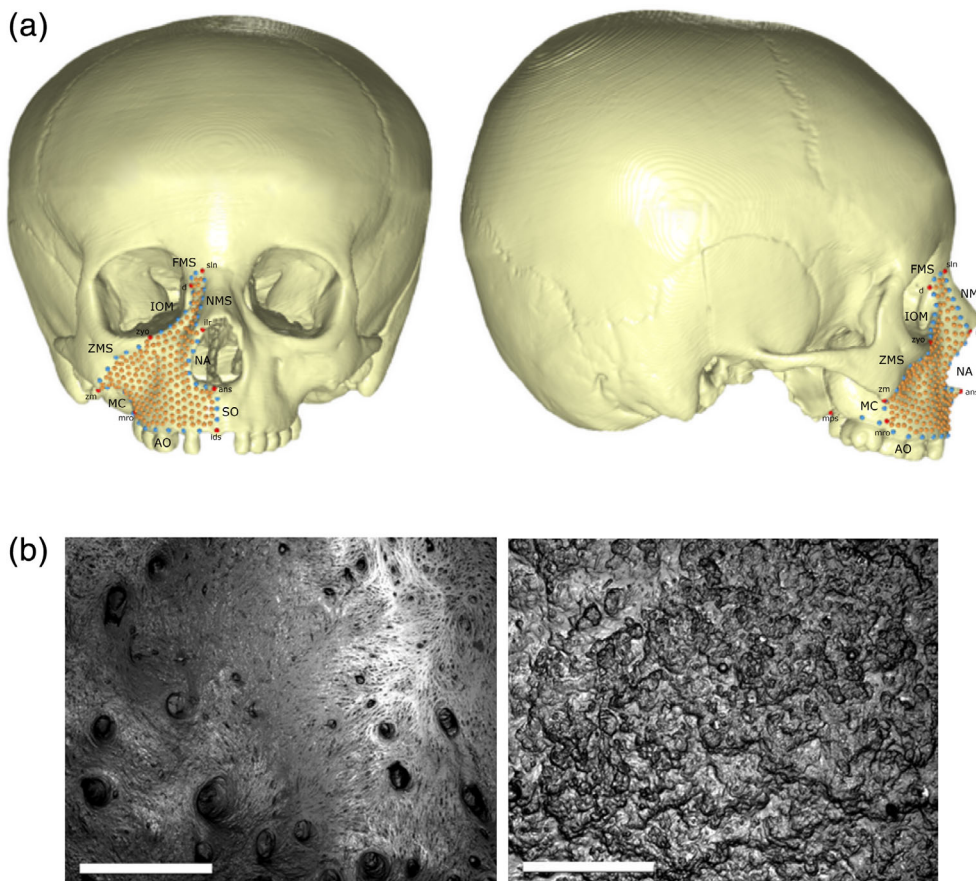


**FIGURE 1** (a) Template of the right maxilla showing 249 landmarks (red dots) and semilandmarks (curve: blue dots; surface: orange dots). Names and definitions of fixed landmarks and curves semilandmarks are given in Table 2. (b) Examples of bone formation (left) and bone resorption (right). Formation is characterized by collagen fibers that are mineralized and visible on dry bones as elongated structures. Scale bar: 1 mm. Bone resorption is detectable by the presence of small depressions, called Howship's lacunae. Scale bar: 500  $\mu$ m

## Developmental simulations

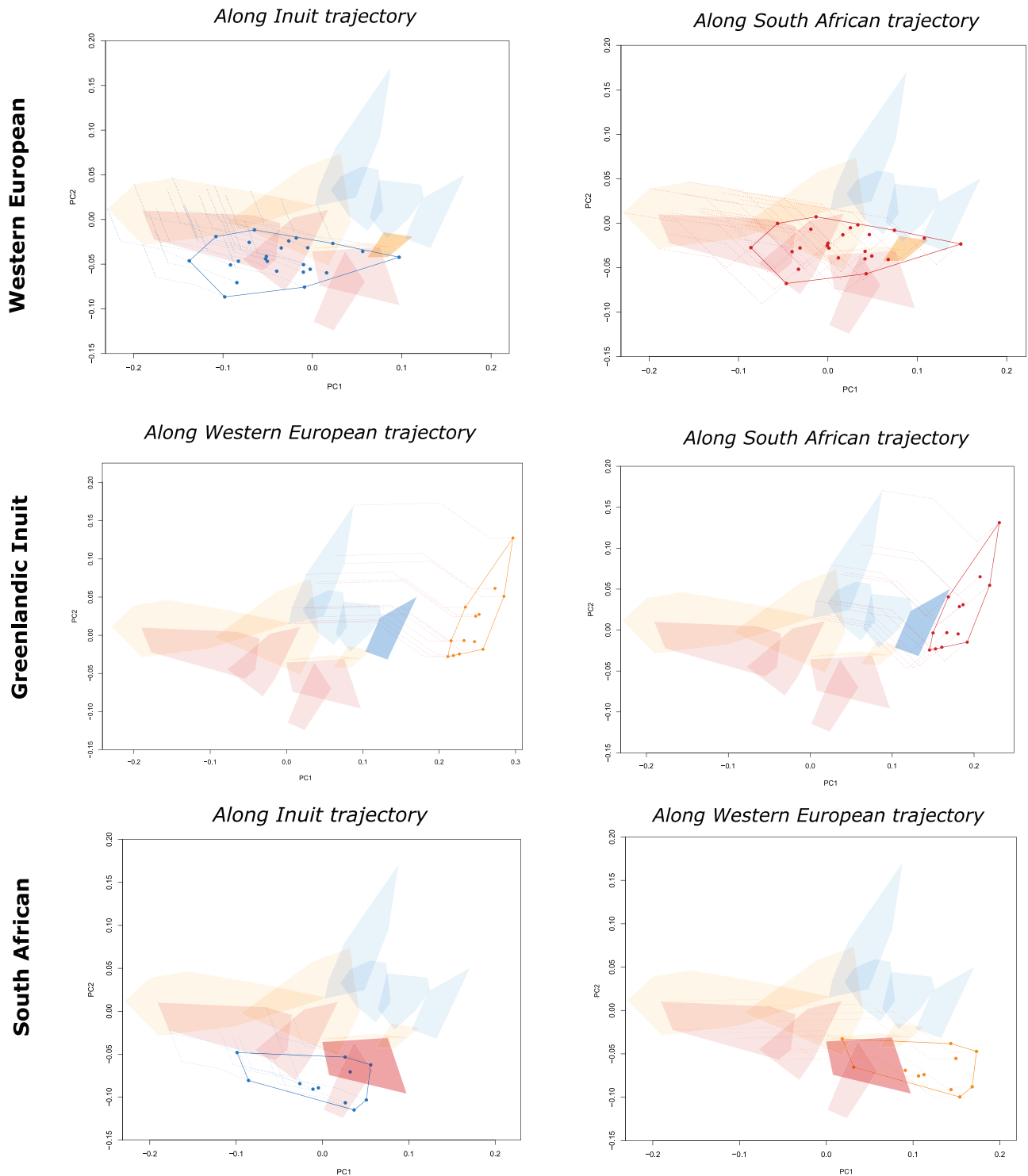


**FIGURE 2** Developmental simulations. Top: Western European AG 1 individuals simulated along the Greenlandic Inuit (left) and South African (right) trajectories; Middle: Greenlandic Inuit AG 1 individuals simulated along the Western European (left) and South African (right) trajectories; Bottom: South African AG 1 individuals simulated along the Greenlandic Inuit (left) and Western European (right) trajectories. Each individual's trajectory is represented as a dotted line. Simulated individuals are shown as dots in a lined convex hull. Both lines and dots are shown in the color of the population for which the trajectory was used (e.g., Western Europeans and South Africans simulated along the Greenlandic Inuit trajectory are shown in blue). Each age group is represented by a filled convex hull in the color of the population (orange: Western European, blue: Greenlandic Inuit, red: South African). Non-simulated adults are shown in a dark shade convex hull

trajectories in a multivariate context. The simulated individuals were compared in a PCA to the non-simulated adults, first within one population (the Western European, as it is the most well-represented of the sample) to test the method, then between populations. If the simulated adults plot close to the non-simulated ones of their own population, then the trajectories are interchangeable. In the opposite case, the trajectories differ between populations (Neubauer et al., 2010).

Intra-population developmental differences across age groups were then visualized with the use of heat maps (Schlager, Profico, Di Vincenzo, & Manzi, 2018). First, independent GPAs were performed on each population to ensure that population differences do not influence the results. The mean shape of each age group was computed using the Procrustes coordinates. A mesh was then warped onto each mean shape using a TPS interpolation. Euclidean distances between two meshes of subsequent age group means (AG 1 and 2 [AG 1-2]; AG 2 and 3 [AG 2-3]; AG 3 and 4 [AG 3-4]) was calculated using a k-dimensional tree search for closest triangles (Schlager, 2017) from the

older to the younger age group. The distances are shown on a map as a color scale of maximum and minimum distances between meshes (a range of 2 and -2, respectively). Positive distances (from 0 to 2) are shown in warm colors, and are interpreted as an anterior displacement of the bone. Similarly, negative distances (from -2 to 0) are shown in cold colors, and are interpreted as a posterior displacement.

## 2.2.2 | Quantification and visualization of the bone modeling patterns

For the surface histology analysis, a grid of 5 × 5 mm squares was drawn on each cast (Martinez-Maza, Rosas, & Nieto-Diaz, 2013). The observations were made using an automated digital microscope (SmartZoom 5, Carl Zeiss Microscopy, Jena, Germany) with a 1.6x PlanApo D objective (zoom: ×34). Bone formation results from the activity of the osteoblasts that produce collagen fibers, identifiable as elongated structures on the

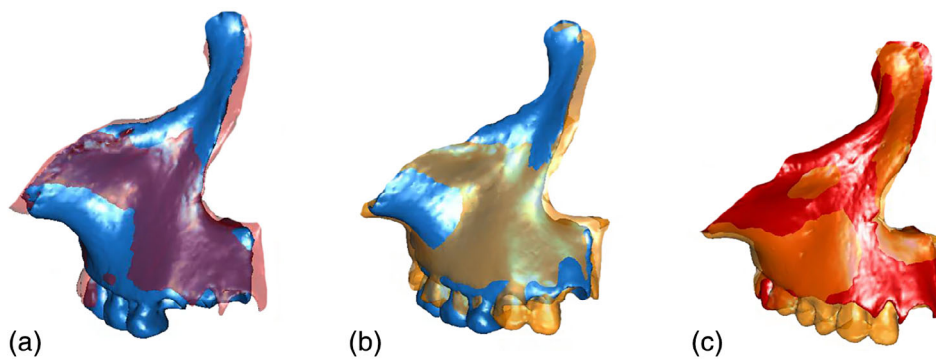


**FIGURE 3** Shape differences between populations visualized by superimpositions of the mean shapes. A: Greenlandic Inuit (blue) and South African (red); Greenlandic Inuit (blue) and Western European (orange); C: Western European (orange) and South African (red)

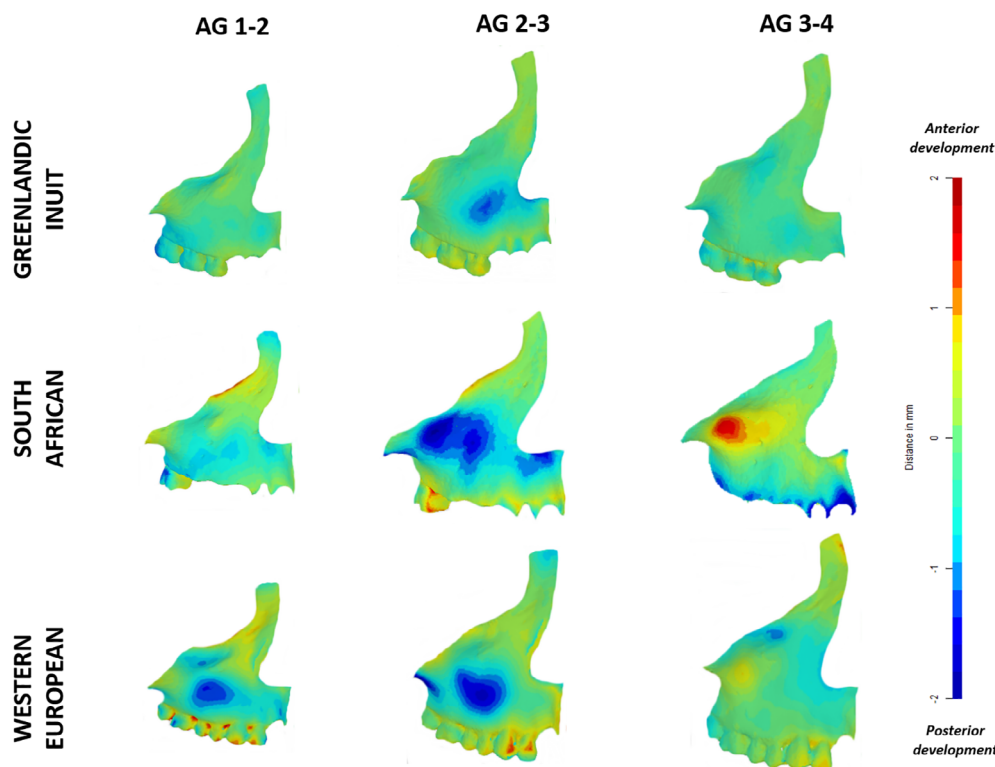


**FIGURE 4** Heat maps showing morphological differences between AG 1 and 2 (AG 1-2), AG 2 and 3 (AG 2-3), and AG 3 and 4 (AG 3-4) for all populations. The differences are calculated as the closest distances between two meshes, which were first warped onto their corresponding mean configuration using a TPS interpolation (after independent GPA alignments for each population). Warm colors indicate positive distances, cold colors indicate negative distances. The color scale was set up on a range from -2 (minimum distance) to 2 (maximum distance). Informative data are only considered for the surface in relation to the template, which exclude the teeth

surface (Figure 1b, left). Bone resorption is defined by the digestion of the bone by the osteoclasts, and results in multiple cavities known as Howship's lacunae (Figure 1b, right; Boyde, 1972). We analyzed each square and recorded the presence of the two activities on handmade maps. When both activities were present, another  $2.5 \times 2.5$  mm grid was drawn within the  $5 \times 5$  mm squares so that pictures at a higher resolution ( $\times 101$ ) could be taken with a PlanApo D  $\times 5$  objective.

Following Schuh et al. (2019), areas of bone resorption were manually selected in order to be quantified using the software ImageJ 1.46r (Schneider, Rasband, & Eliceiri, 2012). A percentage of bone resorption (%BR) for each square of the grid was calculated, as well as the amount of bone resorption per individual by dividing the total %

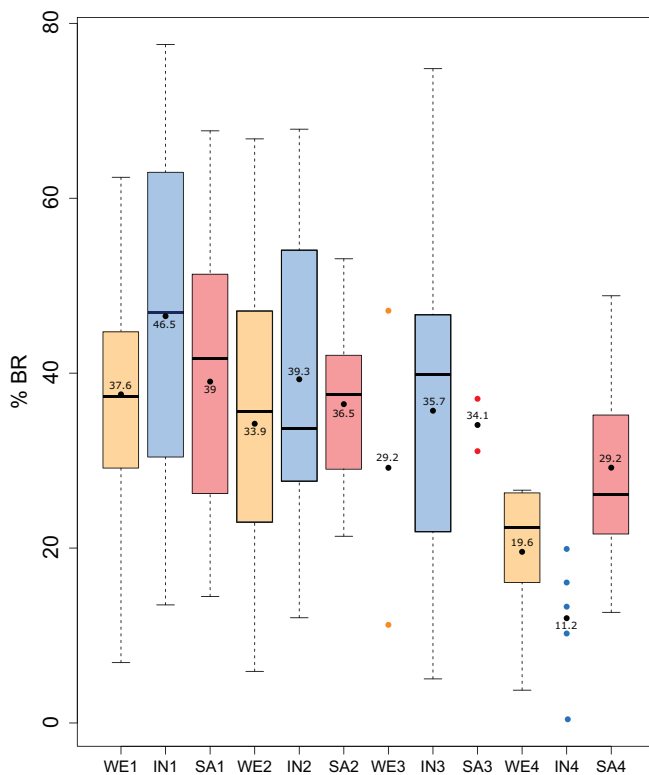


**FIGURE 5** Boxplot representing the variation of the percentages of bone resorption (%BR) in each age group for all populations. Orange: Western European (“WE1”, “WE2”, “WE3”, “WE4”); blue: Greenlandic Inuit (“IN1”, “IN2”, “IN3”, “IN4”); red: South African (“SA1”, “SA2”, “SA3”, “SA4”). Age groups' sizes equal to or less than five individuals were represented by dots in the corresponding population color. Each mean %BR is indicated as a black dot

BR by the total surface area of the bone. From these results, mean % BR and standard deviation were calculated for each age group. In order to compare and visualize the bone modeling patterns between populations, digital maps were computed for each individual in RStudio. The %BR at each square was associated with a color: low values of bone resorption were represented by warm colors, while high values were represented by cold colors. Areas with low amounts of bone resorption are represented by predominant amounts of bone formation; however, this analysis does not distinguish between highly active (as seen in young individuals) and quiescent (as seen in adults) bone formation. To make the comparison between the maps possible (as size differences exist between young and older individuals), scaling to a standardized grid of  $8 \times 8$  squares was performed in R (see Schuh et al., 2019 for a detailed description of the method). We then computed mean bone modeling maps per age group by calculating the average %BR at each square, excluding missing values. In order to visualize both changes in shape together with the bone modeling patterns, each mean bone modeling map was warped onto the 3D surface of its corresponding mean shape in Geomagic® Studio (Research Triangle Park, NC). Population similarities in the bone modeling patterns were tested for the age groups that present a sufficient number of individuals (i.e., AG 1 and 2) using a PERMANOVA (1,000 iterations). Moreover, in order to test if population differences are found in different areas of the maxilla, we performed a MANOVA on each square of the grid, followed by a Bonferroni correction of the  $p$ -values.

### 2.2.3 | Joint analysis between bone modeling and morphological data

Although differences and/or similarities in the bone modeling patterns might explain the variation observed at the morphological scale, the covariation between maxillary morphology and bone modeling might differ between human populations. Thus, we carried out two-block Partial Least squares (PLS) analyses (Rohlf & Corti, 2000) on the bone modeling data and the Procrustes coordinates (see Mayer, Metscher, Müller, and Mitteroecker (2014) as well as Schuh et al. (2019) for more details on the method). The PLS analysis computes pairs of linear combinations (called singular warps, “SW”; Bookstein et al., 2003) that account for the maximum of covariance between two blocks using the covariance matrix. Different PLS analyses were performed on the pooled sample to investigate general trends of covariation, and for each

**TABLE 3** Mean percentage and SD for each age group and population, associated to Figure 5

Age group	Western European		Greenlandic Inuit		South African	
	Mean	SD	Mean	SD	Mean	SD
1	37.6 (24)	13.9	46.5 (13)	19.9	39 (11)	18
2	34.2 (27)	16.1	39.3 (15)	18.7	33.9 (8)	10.6
3	29.8 (2)	25.4	35.7 (15)	19.1	29.2 (2)	4.2
4	19.6 (6)	8.6	11.2 (5)	7.4	19.6 (10)	12.6

Note: The number of individuals is given in parenthesis after the mean.

population separately (to avoid the influence of a group on the others). Missing values were first estimated using a regularized iterative PCA algorithm of the *missMDA* package (Josse & Husson, 2016). After this step, only 32 squares (variables) were kept. To correct for the effect of size, we computed a multivariate linear regression of the shape coordinates on the natural logarithm of the centroid size and performed another two-block PLS analysis between the shape residuals and the bone modeling data including all populations. The significance of each singular value was assessed using a permutation test (1,000 iterations).

### 3 | RESULTS

#### 3.1 | Developmental trajectories and patterns of shape changes

The developmental simulations are shown in Figure 2 (see also Supporting Information S1). Overall, all simulated individuals plot away from the non-simulated ones, implying different developmental trajectories for each population. In both cases, the simulated Inuit individuals from AG 1 result in an elongated trajectory along PC1 (shifted toward the positive values), although less elongated when following a South African trajectory. Similarly, South African individuals simulated along the Western European trajectory are shifted toward the positive values along PC 1, while Western Europeans simulated along the South African trajectory are shifted toward the negative values along PC 1, resulting in a shorter trajectory. Finally, both South Africans and Western Europeans, when simulated along the Inuit

trajectory, are shifted toward the negative values (implying a shortened trajectory) as well as moved toward the negative values on PC 2 (implying a change in direction). Shape differences between the three populations are shown in Figure 3. The Inuit maxilla is consistently shorter mediolaterally, both in the maxillary arcade and the frontal process that is more elongated superoinferiorly. South Africans are slightly more projected in the anterior maxilla, and Western Europeans show a more anteriorly developed anterior nasal spine (ANS).

Figure 4 shows the heat maps computed between age group means' Procrustes coordinates, thus showing the developmental (or shape) differences between two pairs of age group means (AG 1-2, 2-3, and 3-4). Overall, in all populations a posterior displacement (cold colors) is found in the inferior orbital ridge, the canine area, and in the anterior maxilla while a slight anterior displacement is found in the frontal process (warm colors). This suggests a shared general pattern of development between the three populations; however, slight differences can be observed. While in Inuit and South Africans the differences shown in AG 1-2 are small (the distance is close to 0 mm), Western Europeans show a marked

**TABLE 4** Degree of freedom (*df*), coefficient of determination ( $R^2$ ) and *p*-values of the PERMANOVA testing for population similarities in the bone modeling patterns at each age group, considered significant for  $p \leq .05$

Age group	<i>df</i>	$R^2$	<i>p</i> -value
1	2	0.07	.06
2	2	0.07	.05

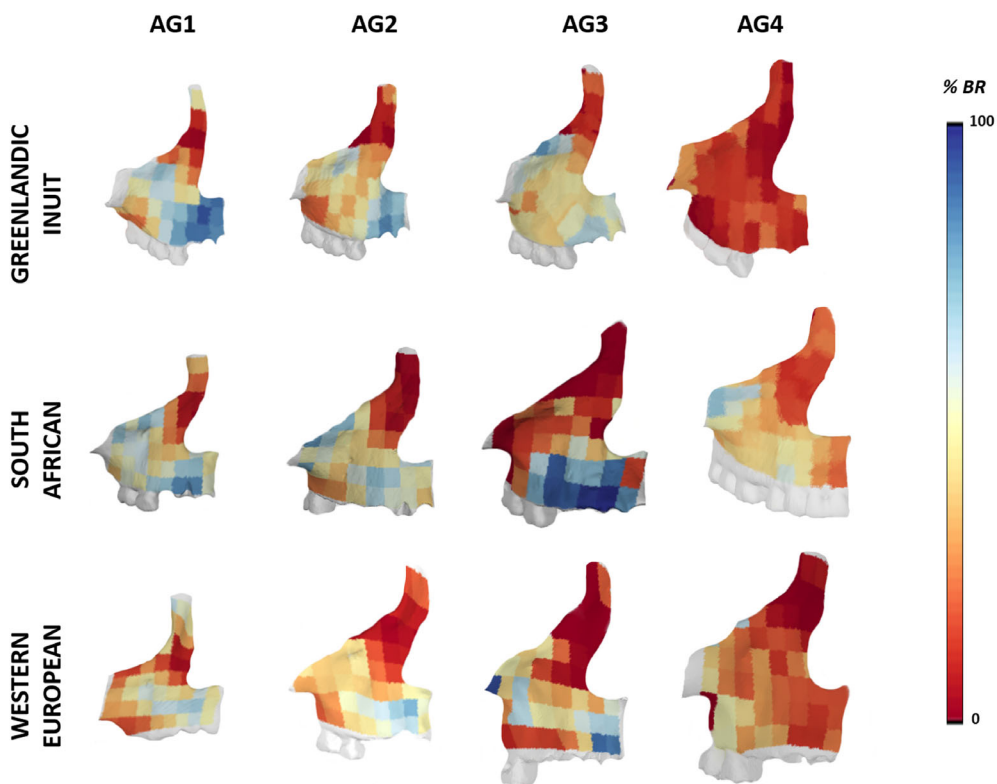


**FIGURE 6** Maps showing the average bone modeling pattern at each age group and for each population. Cold colors (between 50 and 100%) indicate high amounts of bone resorption while warm colors (between 0 and 50%) indicate low amounts of bone resorption (i.e., predominant bone formation, whether it is in an active or quiescent state). Each map was projected onto the mean shape of the corresponding age group

posterior displacement in the canine fossa. Most evident shape differences are found in AG 2–3 in all populations, with a posterior displacement located in the canine fossa. Finally, developmental differences between AG 3 and 4 appear very slight in both Inuit and Western Europeans. South Africans show a marked anterior displacement in the infraorbital region.

### 3.2 | Patterns of bone modeling across human populations

A percentage of bone resorption was obtained for each individual, and average %BR were calculated for each age group. Results are represented as boxplots in Figure 5, and means and standard deviations are shown in Table 3. Overall, a similar pattern is observed in each population, showing a progressive decrease in the %BR, with the youngest age groups showing higher %BR on average than the adults (between 29.2 and 46.5% against 12 and 29.2%). Western Europeans show on average 10% less bone resorption than the two other populations, except in AG 4. The average %BR in South African adults is higher than in the two other populations (29.2% against 19.6 and 12%). Standard deviations are generally higher in AG 1 and 2 (ranging from 13.9 to 18.7) compared with AG 4 (ranging from 7.4 to 12.6). The Western European and South African AG 3 show the highest and lowest values (25.4 and 4.2 respectively;  $n = 2$  in each population).

We computed the average bone modeling maps for each age group and projected them onto their corresponding mean shapes (Figure 6). We observed a general dichotomy of the bone, with the frontal process being mostly represented by bone formation (the %BR ranging from 0 to less than 50%), and the zygomatic process and maxillary arcade mostly resorptive (with percentages ranging from

minimum 50 to 100%). Each population expresses differences in the location of bone resorption from early on. Western Europeans and South Africans show more resorption on the canine bulb and the canine fossa, with South Africans expressing also more resorption around the orbital ridge. The Inuit pattern expresses a maximum %BR in the anterior part of the maxillary arcade (on top of the incisors). Results from the PERMANOVA testing for population similarities in the bone modeling patterns are given in Table 4. Only AG 2 shows significantly different mean values in the %BR ( $p \leq .05$ ). In each population, the bone modeling pattern expressed in AG 1 is repeated until at least AG 3. The decrease of %BR observed in Figure 5 in AG 4 is well represented by the adult bone modeling maps that express low amounts of bone resorption. However, compared with the two other populations adult South Africans seem to maintain the pattern found in the subadults by expressing more resorption in the maxillary arcade.

Figure 7 shows the results of the MANOVA, testing for statistical differences in the bone modeling patterns at each square for each age group (see also Supporting Information S2). In AG 1, significant differences are located mostly at the bottom of the frontal process, along the zygomaticomaxillary suture and close to the inter-maxillary suture (in the anterior maxilla). In AG 2, the bone modeling pattern at the bottom and top (close to the frontomaxillary suture) of the frontal process were significantly different between populations, as well as along the zygomaticomaxillary suture.

### 3.3 | Comparison between the micro- and macroscopic changes

Figure 8 shows the PLS analysis between the Procrustes shape coordinates and the bone modeling data in all populations. The first pair of

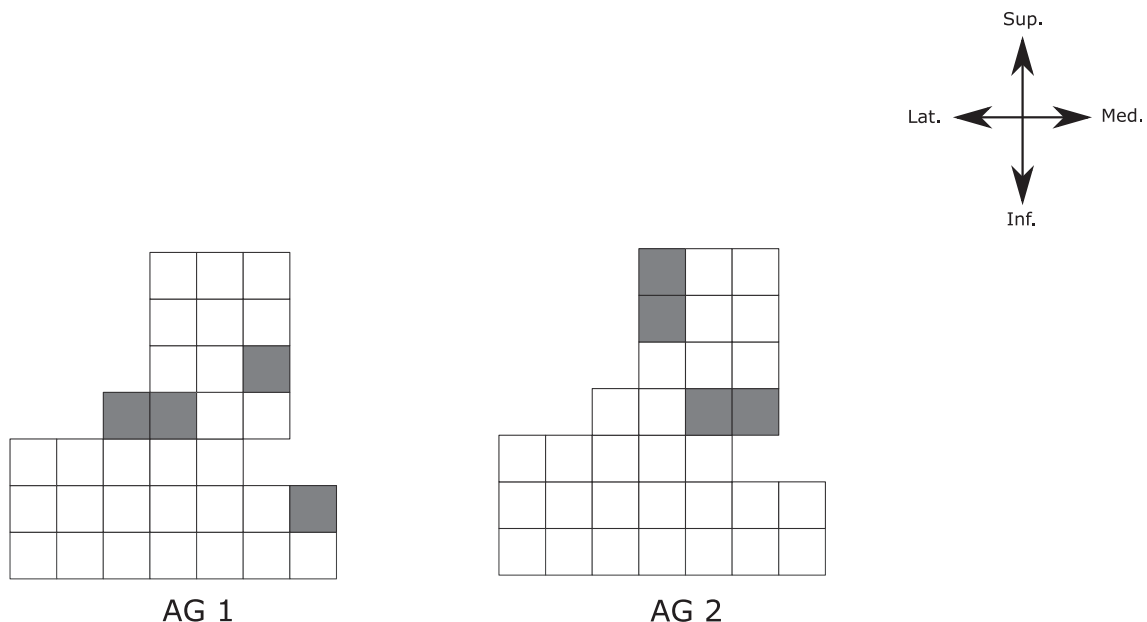


**FIGURE 7** Maps showing the results of the MANOVA testing for significant differences between populations at each square of the grid. Gray squares show where the results are significant (for  $p \leq .05$ )

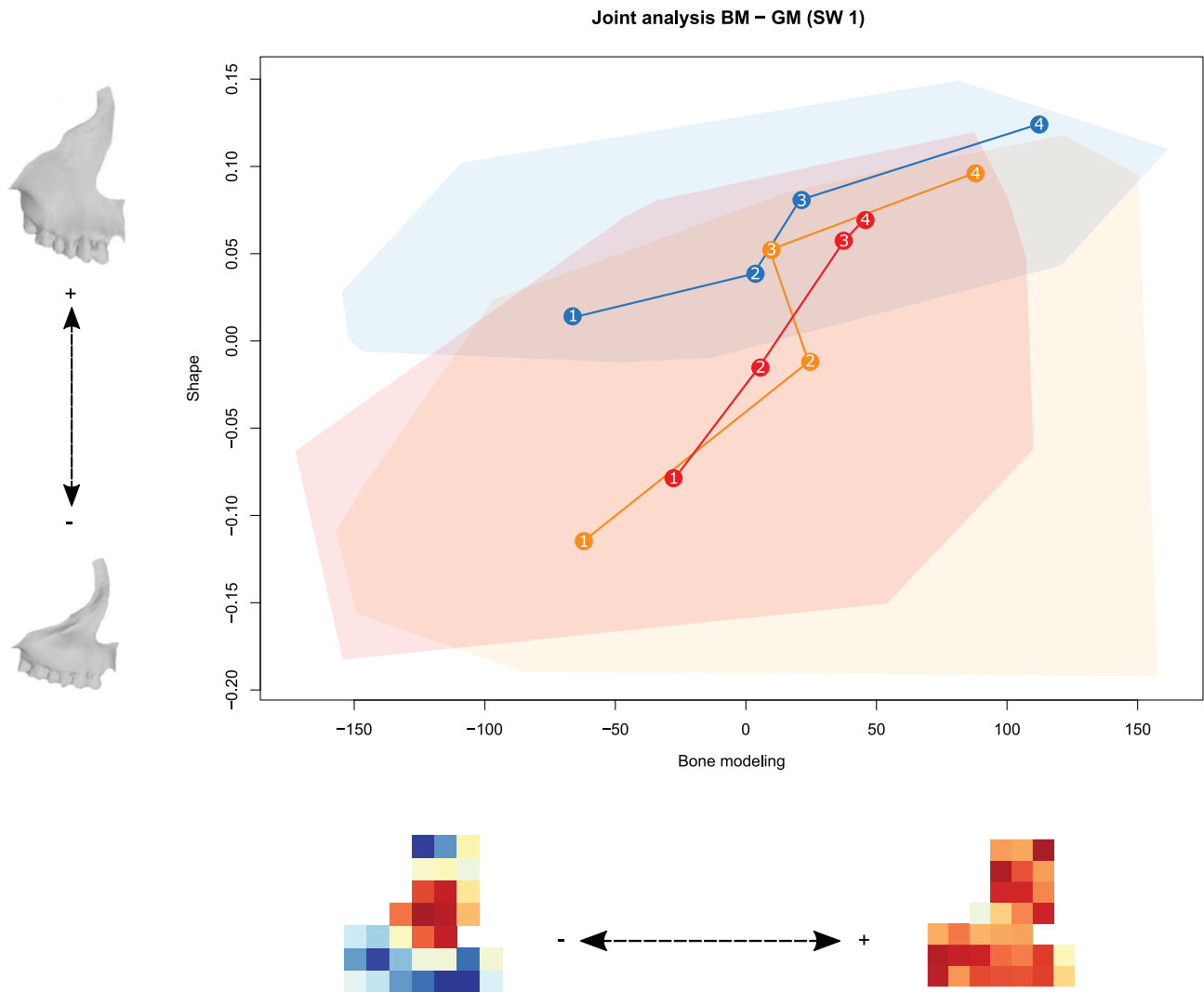


**FIGURE 8** Two-block partial least square (PLS) analysis between the bone modeling and morphological (shape) data (SW 1). X-axis: bone modeling data; y-axis: morphological data, represented by the Procrustes shape coordinates. Each population is represented by a convex hull (blue: Greenlandic Inuit; red: South African; orange: Western European). Age group means are represented by dots and corresponding numbers. Solid lines connect the subsequent means

**TABLE 5** Percentages of total covariance, correlation coefficient and *p*-value, computed for the first singular warp (SW 1) of the PLS analysis between Procrustes shape coordinates and the corresponding bone modeling patterns on all populations

	% Total covariance	Correlation coefficient (R)	<i>p</i> -value
SW1	73	0.42	.001

singular warps (SW 1) explains 75.6% of the total covariance between the two blocks (correlation coefficient: 0.42; Table 5). The x-axis separates the younger and older individuals (although more variation is seen in Western Europeans in the youngest age groups). On the y-axis, a shape change of the orbital ridge is observed. Although a high overlap is observed, the Inuit AG 1 individuals plot toward the positive values while the other two populations AG 1 plot toward the negative values. Changes on both axes toward

positive values respectively correspond to a decrease in the bone resorption associated with an increase in height and width of the bone, particularly in the frontal process. Overall, the trajectories show a similar pattern of covariation between shape and bone modeling from AG 2 (corresponding to the completion of the M1) to AG 4 (adulthood), although the Inuit (in blue) show the most different trajectory (more constant, implying less shape change). They also show less overlap with the other two populations and less overall variability.

To avoid the influence of each population on the others, separate PLS analyses were performed (Figure 9; Table 6). As before, a similar pattern is observed in all populations, with the highest variability observed in the youngest individuals (AG 1) and the lowest in the adults (AG 4). This corresponds to a general decrease in bone resorption in all populations, and an increase in height and width of the maxilla. The distribution of bone resorption, although overall very similar,

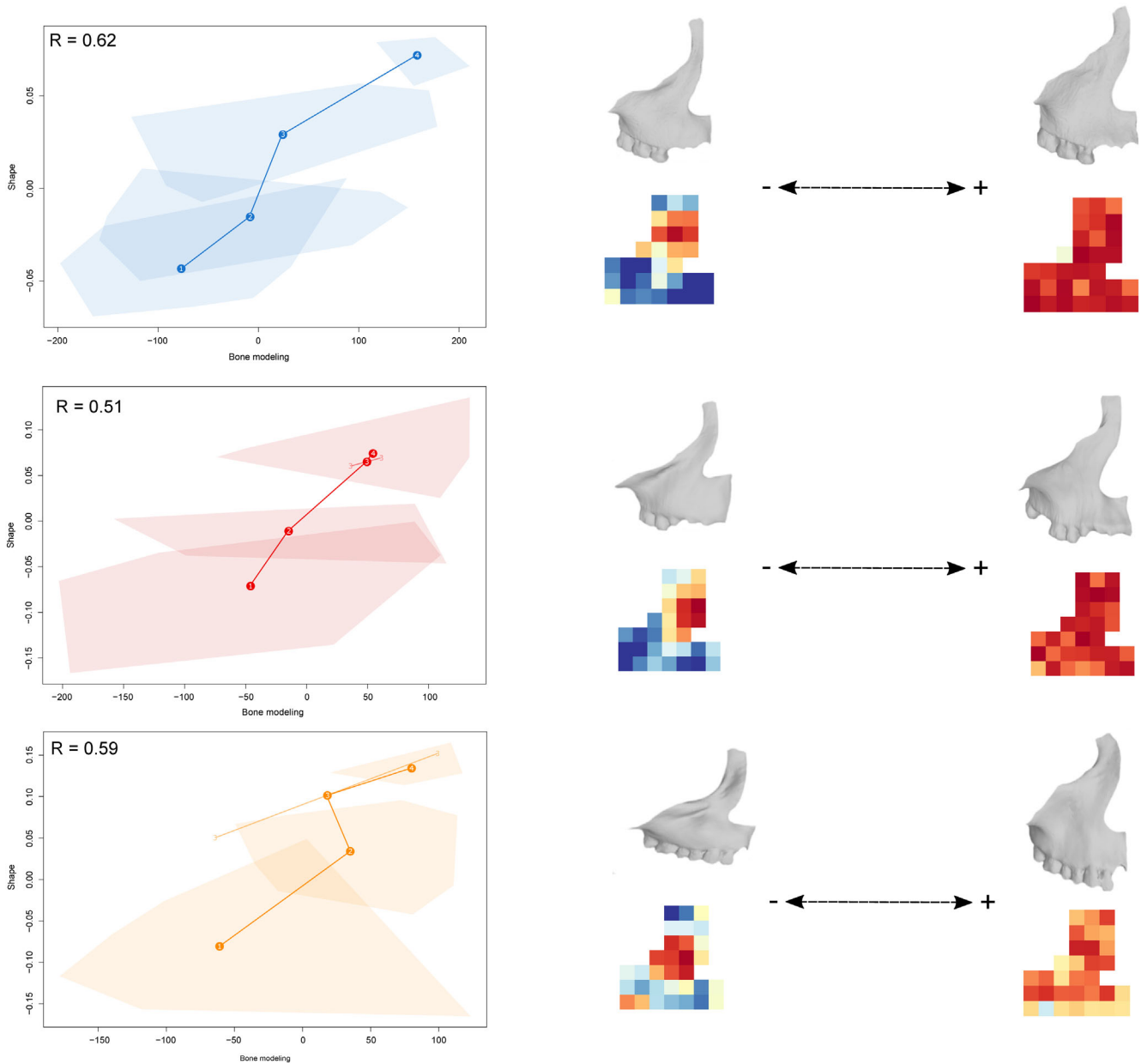


**FIGURE 9** Two-block partial least square (PLS) analyses between the bone modeling and morphological (shape) data for each population (SW 1). Left: plots for each population; (a) Greenlandic Inuit, (b) South African, (c) Western European. Age groups are delimited by convex hulls within each plot. Age group means are represented by dots and corresponding numbers. Solid lines connect the subsequent means. The Western European and South African AG 3 are only represented by two individuals, connected by a solid line and shown in the graph as numbers. Right: visualizations of the shape and bone modeling changes corresponding to SW 1 positive and negative extremes

**TABLE 6** Percentages of total covariance, correlation coefficients and *p*-values, computed for the first singular warp (SW 1) of the PLS analyses between Procrustes shape coordinates and the corresponding bone modeling data for all age groups in each population, separately

	% Total covariance	Correlation coefficient (R)	<i>p</i> -value
Greenlandic Inuit	73	0.62	.001
Western European	85.2	0.59	.001
South African	74.2	0.51	.06

shows slight differences in each population that are linked to shape differences, mostly in the frontal process and the projection of the anterior maxilla.

#### 4 | DISCUSSION

We investigated the intraspecific variability of the bone modeling patterns in the maxillae of three human populations, and compared the expression of their microscopic patterns to the development of their macroscale features during ontogeny.

## 4.1 | Maxillary morphology and ontogenetic patterns

Previous studies have already shown that population differences in facial morphology develop early, possibly prenatally (Bastir, O'Higgins, & Rosas, 2007; Bulygina et al., 2006; Freidline et al., 2015; Sardi & Ramirez-Rozzi, 2012; Vidarsdóttir et al., 2002; Viðarsdóttir & O'Higgins, 2003); however, the morphological variation in prenatal stages has only been investigated in few studies (Mooney & Siegel, 1986; Weinberg, 2005; Morimoto, Ogihara, Katayama, & Shiota, 2008; Nicholas, 2016). Using geometric morphometric techniques, Nicholas (2016) found shape differences in the fetal maxilla between African- and European-Americans as early as the second trimester. The results of our morphological analysis further support these findings, as shape differences between the three populations can be observed already around birth (Figure 2). The developmental simulations performed on each population showed that they are not interchangeable, as differences in the trajectory sizes, shapes, and magnitudes could be observed (Adams & Collyer, 2009). At a similar age group, the Inuit maxilla is always larger and more developmentally advanced, and the shorter length of their developmental trajectory suggests less postnatal shape changes than in the two other populations. When interchanged, the South African and Western European trajectories mostly result in a displacement of the simulated adults along PC1, suggesting differences in the amount of shape change along a largely similar developmental trajectory in comparison to the Inuit. All of this suggests differential pre-, as well as postnatal, rates and/or timings of development as already suggested by other studies (Sardi & Ramirez-Rozzi, 2012; Vidarsdóttir et al., 2002). Freidline et al. (2015) who analyzed the whole face and employed similar populations as in this study, demonstrated as well that facial morphological variability arises from differential developmental patterns, mostly driven by size differences.

The heat maps in Figure 4 were computed to compare patterns of shape differences between subsequent age groups in the three populations. These shape differences were interpreted as the general, main displacements of the bone between two subsequent age groups (as the bones are continuously growing in all directions; Enlow, 1966). All populations show a similar general pattern of displacements between age groups, with a main anterior displacement in the frontal process and most of the posterior displacement observed in the canine fossa. This corresponds to areas that are predominantly forming and resorptive throughout ontogeny, respectively (although bone resorption is expressed on intermediate levels; see the mean bone modeling maps in Figure 6). Inuit show less posterior displacement in the canine fossa, which can explain their midfacial flatness (Hennessy & Stringer, 2002); however, they do not differ from the other populations in the anterior maxilla where we expected the most differences (see discussion below). Interestingly, the heat maps all indicate a rather late development of the canine fossa, except between the Western European AG 1 and 2 that already show a marked posterior displacement compared with the two other populations. The higher number of very young individuals in this population AG

1 might explain this difference (such as in the South African AG 3–4 represented by only two individuals).

## 4.2 | Variability of the bone modeling patterns

The analysis of bone resorption showed comparable distributions and means in the %BR in all populations (Figure 5, Table 3), although Inuit possess slightly more resorption on average. We found a shared general bone modeling pattern in all three populations (Figure 6), with predominant bone formation in the frontal process and bone resorption in the maxillary arcade as shown in former studies (Brachetta-Aporta, Gonzalez, & Bernal, 2019a; Enlow & Bang, 1965; Kurihara, Enlow, & Rangel, 1980; Martinez-Maza et al., 2013; Schuh et al., 2019). However, we did find significant statistical differences in bone modeling between the three populations (Table 4). These differences have been highlighted in the location of bone resorption (Figures 6 and 7), particularly in the Inuit pattern that shows a more anterior area of bone resorption (on top of the incisors' roots); this observation can already be made from AG 1 as shown by the results of the MANOVA (Figure 7, Supporting Information S2). Both Inuit and Western Europeans possess taller and narrower nasal regions than South Africans, and our results seem to suggest that significant differences in bone modeling exist in this region that comprises the frontal process and the anterior maxilla (Figure 7; also shown at the morphological level in Figure 3); although this would have to be tested on more individuals. Moreover, we observed that population-specific bone modeling patterns are present since early stages, and maintained throughout ontogeny until at least adolescence (AG 3 in our sample); however, this could not be tested statistically. Yet with this observation, we can still conclude that the expression of bone resorption is likely a highly genetically controlled process, and its location on bone surfaces underlies the development of a specific form. The repetition of a bone modeling pattern within a group/species may be indicative of developmental canalization (Hallgrímsson, Willmore, & Hall, 2002; Waddington, 1942).

The progressive decrease observed throughout ontogeny in the percentages of bone resorption (attaining lower values and less variation in adults) implies lowered osteoblastic and osteoclastic activities that follow a general decrease in the growth rate of the face in later ontogeny (Bastir, Rosas, & O'Higgins, 2006). McCollum (2008) described different types of bone resorption, such as "aggressive" and "skimming." Skimming resorption affects the boneless, and according to our data, is more predominant in adults, which again suggests differences in cellular rates between the latter and the subadults. Bone resorption is also slightly less predictable, and when present as small-localized fields, may indicate areas of bone remodeling in response to biomechanical demands. Interestingly, adult South Africans in our sample show a higher %BR than the two other populations; this might be due to the composition of this age group (with younger adults), but demonstrates that bone modeling can stay as active as during childhood until at least early adulthood. In a study from 2013, Martinez-Maza and colleagues found differences in the bone modeling patterns

of subadult and adult Western Europeans. According to the authors, resorption in adults is restricted to the posterior canine region. They concluded that these differences result in a change of the general facial growth vector, from a mainly forward/downward vector found in subadults to a unique forward direction in adults. Although a similar finding is shown in our adult Western Europeans ( $n = 6$ ; Figure 6), we generally observed that areas affected by bone resorption in adults are comparable to those observed in subadults, as discussed by Brachetta-Aporta, Gonzalez, and Bernal (2019b). It is thus difficult to conclude whether a significant change in the general direction of growth occurs between the two. Changes in facial size and shape during adulthood have been demonstrated by several studies (Behrents, 1985; Behrents, 2008; Guagliardo, 1982; Hellman, 1927; Israel, 1968, 1977; Williams & Slice, 2010). These changes can be found in both the soft tissues (Behrents, 2008; Windhager et al., 2019) and bones (Albert, Ricanek, & Patterson, 2007). Williams and Slice (2010) observed a decrease in facial height in the superior-inferior direction, as well as a lateral expansion associated with age. The authors observed shape changes in the orbital, zygomatic, and maxillary alveolar regions, with variations dependent of the sex and/or ethnic origin studied. Whether they relate to bone modeling changes in elderly individuals remains to be tested.

### 4.3 | Facial ontogenetic patterns at the micro- and macroscopic scale

Inuit possess distinct external and internal nasal shapes that have been linked to an adaptation to cold climates (Maddux et al., 2017), and different analyses in this study suggest that bone modeling patterns of this area slightly differ between populations (Figures 6 and 7). Apart from the nasal region, morphological adaptation to climate has proved complex in human populations, as their association can only be highlighted in cases of extremely cold environments (Evtsev et al., 2013; Harvati & Weaver, 2006). South Africans who possess rather short and broad frontal processes (Figure 3) express slightly more bone formation in this area, while Inuit and Western Europeans who possess more elongated frontal processes show resorption until at least AG 3. Moreover, the anterior nasal spine (ANS), a unique human morphological feature (Ashley-Montagu, 1935), is known to show population differences in its development (Mooney & Siegel, 1986). In this study, the ANS region is often resorptive in subadults, particularly in Inuit who consistently show a reduction in the size of the ANS compared to the other two populations (Figure 3). Thus, the forward development of the ANS might depend on the ratio between bone formation and resorption to which it is subjected during ontogeny. This also shows the importance of considering different human groups in the analysis of intraspecific variation of the bone modeling patterns, as previous work with reduced sample sizes found mostly bone formation in this region (Enlow & Bang, 1965). Moreover, the location of the maximum %BR (in the anterior maxilla) is unique to the Inuit sample of this study (Figure 6). According to Hylander (1977), the Inuit face is well adapted to high load demands, as many of their

facial features facilitate the dissipation of vertical occlusion forces such as a more anteriorly positioned postorbital bar, an anterior root of the zygomatic bone, and hypertrophied masseter muscles. Coon (1962) also noted an anterior displacement of the temporalis (that is on average larger than in other populations) and masseter. Toro-Ibacache, Zapata Muñoz, and O'Higgins (2016) observed lowered peak strains in more vertical faces, which could apply to the Inuit as their facial prognathism is reduced compared with other populations. Thus, a more anterior resorptive field (on the incisors) as well as a more lateral development of the facial components might be linked to their facial flatness, whereas a more lateral resorptive field (on the canine fossa) might create a more concave maxilla as seen in Western Europeans and South Africans. We thus propose that the location of bone resorption on the bone may be a response to larger-scale ontogenetic patterns (such as integration patterns within the skull), and result from compensatory mechanisms as proposed by other authors (Mitteroecker et al., 2020; O'Higgins, Bromage, Johnson, Moore, & McPhie, 1991). Finally, the analysis of covariation between the shape residuals and the bone modeling patterns again highlighted subtle population differences (Figure 8, Supporting Information S3 and S4), while overall, a similar general pattern is found (Figure 9). This suggests that only slight, but significant changes in the location of the bone modeling patterns participate in the shape differences observed in human populations.

## 5 | CONCLUSION

This study investigates for the first time the bone modeling patterns of several geographically distinct human populations, and shows the importance of considering a large, diverse sample to try to better represent the variation at the species level. We showed that although *Homo sapiens* express overall similar general maxillary ontogenetic bone modeling patterns and shape changes, population-specific differences can be found at both levels. These are expressed in the rates and timing of development that occur pre- and post-natally, in the complex integration of the face with other cranial components during ontogeny as well as in the location of bone resorption (particularly in the nasal region). The subtle discrepancies in the bone modeling patterns observed in this study suggest that shape differences are merely due to differences in rates and/or timings of development (at the cellular level) than differences in the location of bone resorption. Inuit are the most distinct at both levels, showing more advanced maxillary development and a more anteriorly resorptive field, which could explain the horizontal development of their midface. Moreover, this study shows that population-specific bone modeling patterns in *H. sapiens* are maintained throughout ontogeny; and this may apply as well to other hominin species. Although most of the features are established at birth, changes in the bone modeling and morphological patterns observed here highlight the role of later phases of postnatal ontogeny in shaping the human face. Adults show an important reduction in the total percentage of bone resorption, but resorbing areas are found at similar locations than subadults. These results bring new

insights into our knowledge of ontogenetic patterns that lead to morphological variability.

## ACKNOWLEDGMENTS

We would like to thank the two anonymous reviewers for their constructive comments, as well as J.-L. Kahn (Anatomical Institute of the University of Strasbourg, France), H. Coqueugniot (UMR 5199 PACEA, University of Bordeaux, France), C. Feja (University of Leipzig, Germany), N. Lynnerup (Department of Forensic Medicine of the University of Copenhagen, Denmark), the Greenland National Museum (Greenland), W. Seconna (Iziko Museum of Cape Town, South Africa) and V. Gibbons (University of Cape Town, South Africa), D. Morris (McGregor Museum of Kimberley, South Africa), A. Santos (Department of Life Sciences, University of Coimbra, Portugal) and A. Rosas (Department of Paleobiology, MNCN, Madrid, Spain) for giving us access to the collections. We are also grateful to P. Mitteroecker (University of Vienna, Austria) and V. Toro-Ibacache (Faculty of Dentistry, University of Chile, Santiago) for fruitful discussions, and E. Schulz-Kornas (University of Leipzig, Germany) and Heiko Temming (Max Planck Institute for Evolutionary Anthropology, Leipzig, Germany) for technical assistance. This work was funded by the Max Planck Society, and approved by the South African San Council. Open access funding enabled and organized by Projekt DEAL.

## AUTHOR CONTRIBUTIONS

**Alexandra Schuh:** Conceptualization; formal analysis; investigation; methodology; validation; visualization; writing-original draft; writing-review and editing. **Chiara Villa:** Data curation; resources. **Kornelius Kupczik:** Project administration; resources; supervision. **Philipp Gunz:** Formal analysis; supervision; writing-original draft. **Jean-Jacques Hublin:** Funding acquisition. **Sarah Freidline:** Conceptualization; methodology; project administration; supervision; validation; writing-original draft; writing-review and editing.

## CONFLICT OF INTEREST

The authors declare no conflict of interest.

## DATA AVAILABILITY STATEMENT

The data that support the findings of this study are partly available on request from the corresponding author. The data are not publicly available due to ethical restrictions.

## ORCID

Alexandra Schuh  <https://orcid.org/0000-0003-1645-1220>

## REFERENCES

- Adams, D. C., & Collyer, M. L. (2009). A general framework for the analysis of phenotypic trajectories in evolutionary studies. *Evolution: International Journal of Organic Evolution*, 63(5), 1143–1154.
- Albert, A. M., Ricanek, K., & Patterson, E. (2007). A review of the literature on the aging adult skull and face: Implications for forensic science research and applications. *Forensic Science International*, 172(1), 1–9.
- AlQahtani, S. J., Hector, M. P., & Liversidge, H. M. (2010). Brief communication: The London atlas of human tooth development and eruption. *American Journal of Physical Anthropology*, 142(3), 481–490.
- Ashley-Montagu, M. F. (1935). The premaxilla in the primates. *The Quarterly Review of Biology*, 10(1), 32–59.
- Bastir, M., O'Higgins, P., & Rosas, A. (2007). Facial ontogeny in Neanderthals and modern humans. *Proceedings of the Biological Sciences*, 274(1614), 1125–1132.
- Bastir, M., & Rosas, A. (2004). Comparative ontogeny in humans and chimpanzees: Similarities, differences and paradoxes in postnatal growth and development of the skull. *Annals of Anatomy - Anatomischer Anzeiger*, 186(5), 503–509.
- Bastir, M., Rosas, A., & O'Higgins, P. (2006). Craniofacial levels and the morphological maturation of the human skull. *Journal of Anatomy*, 209(5), 637–654.
- Behrents, R. G. (1985). *Growth in the aging craniofacial skeleton* (2nd ed., Vol. Monograph 17). Ann Arbor: University of Michigan.
- Behrents, R. G. (2008). Adult craniofacial growth. In D. H. Enlow & M. G. Hans (Eds.), *Essentials of facial growth* (2nd ed.). USA: Ann Arbor: Needham Press.
- Bookstein, F. L. (1997). Landmark methods for forms without landmarks: Morphometrics of group differences in outline shape. *Medical Image Analysis*, 1(3), 225–243.
- Bookstein, F. L., Gunz, P., Mitteroecker, P., Prossinger, H., Schaefer, K., & Seidler, H. (2003). Cranial integration in homo: Singular warps analysis of the midsagittal plane in ontogeny and evolution. *Journal of Human Evolution*, 44(2), 167–187.
- Boyde, A. (1972). Scanning electron microscope studies of bone. In G. H. Bourne (Ed.), *The biochemistry and physiology of bone*. New York: Academic Press.
- Brachetta-Aporta, N., Gonzalez, P. N., & Bernal, V. (2019a). Variation in facial bone growth remodeling in prehistoric populations from southern South America. *American Journal of Physical Anthropology*, 169(3), 422–434.
- Brachetta-Aporta, N., Gonzalez, P. N., & Bernal, V. (2019b). Integrating data on bone modeling and morphological ontogenetic changes of the maxilla in modern humans. *Annals of Anatomy - Anatomischer Anzeiger*, 222, 12–20.
- Bromage, T. G. (1989). Ontogeny of the early hominin face. *Journal of Human Evolution*, 18, 751–773.
- Bulygina, E., Mitteroecker, P., & Aiello, L. (2006). Ontogeny of facial dimorphism and patterns of individual development within one human population. *American Journal of Physical Anthropology*, 131(3), 432–443.
- Butaric, L. N., & Maddux, S. D. (2016). Morphological Covariation between the maxillary sinus and Midfacial skeleton among sub-Saharan and circumpolar modern humans. *American Journal of Physical Anthropology*, 160(3), 483–497.
- Churchill, S.E., Shackelford, L.L., Georgi, J.N., & Black, M.T. (2004). Morphological variation and airflow dynamics in the human nose. *16(6)*, 625–638.
- Coon, C. (1962). In (Ed.), *The origin of races*. New York: Alfred A. Knopf.
- Coon, C., Garn, S., & Birdsell, J. (1950). In (Ed.), *Races: A study of the problems of race formation in man*, Springfield, Illinois: Charles C. Thomas.
- Cruwys, E. (1988). Morphological variation and wear in teeth of Canadian and Greenland Inuit. *Polar Record*, 24(151), 293–298.
- Cui, Y., & Leclercq, S. (2017). Environment-related variation in the human mid-face. *The Anatomical Record*, 300(1), 238–250.
- Deter, C. A. (2009). Gradients of occlusal wear in hunter-gatherers and agriculturalists. *American Journal of Physical Anthropology*, 138(3), 247–254.
- Enlow, D. H. (1962). A study of the post-Natal growth and remodeling of bone. *American Journal of Anatomy*, 110(2), 79–101.
- Enlow, D. H. (1966). A morphogenetic analysis of facial growth. *American Journal of Orthodontics*, 52(4), 283–299.
- Enlow, D. H., & Bang, D. D. S. (1965). Growth and remodeling of the human maxilla. *American Journal of Orthodontics*, 51(6), 446–464.

- Evteev, A., Cardini, A. L., Morozova, I., & O'Higgins, P. (2013). Extreme climate, rather than population history, explains mid-facial morphology of northern Asians. *American Journal of Physical Anthropology*, 153(3), 449–462.
- Franciscus, R. G., & Long, J. C. (1991). Variation in human nasal height and breadth. *American Journal of Physical Anthropology*, 85(4), 419–427.
- Freidline, S. E., Gunz, P., & Hublin, J. J. (2015). Ontogenetic and static allometry in the human face: Contrasting Khoisan and Inuit. *American Journal of Physical Anthropology*, 158(1), 116–131.
- Freidline, S. E., Martinez-Maza, C., Gunz, P., & Hublin, J. J. (2016). Exploring modern human facial growth at the micro- and macroscopic levels. Christopher J. Percival & Joan T. Richtsmeier In *Buidling bones*. Cambridge: Cambridge University Press.
- Frost, H. M. (1987). Bone "mass" and the "mechanostat": A proposal. *The Anatomical Record*, 219(1), 1–9.
- Gonzalez-Jose, R., Ramirez-Rozzi, F., Sardi, M., Martinez-Abadias, N., Hernandez, M., & Pucciarelli, H. M. (2005). Functional-cranial approach to the influence of economic strategy on skull morphology. *American Journal of Physical Anthropology*, 128(4), 757–771.
- Guagliardo, M. (1982). *Craniofacial structure, aging and dental function: Their relationships in adult human skeletal series*. (doctoral dissertation). University of Tennessee, Knoxville
- Gunz, P., & Mitteroecker, P. (2013). Semilandmarks: A method for quantifying curves and surfaces. *Hystrix, the Italian Journal of Mammalogy*, 24(1), 103–109.
- Gunz, P., Mitteroecker, P., & Bookstein, F. (2005). Semilandmarks in three dimensions. In D. E. Slice (Ed.), *Modern Morphometrics in physical Anthropology*. New York: Kluwer Press.
- Gunz, P., Neubauer, S., Maureille, B., & Hublin, J.-J. (2010). Brain development after birth differs between Neanderthals and modern humans. *Current Biology*, 20(21), R921–R922.
- Hallgrímsson, B., Willmore, K., & Hall, B. K. (2002). Canalization, developmental stability, and morphological integration in primate limbs. *American Journal of Physical Anthropology*, Suppl 35, 131–158.
- Hanihara, T. (1996). Comparison of craniofacial features of major human groups. *American Journal of Physical Anthropology*, 99(3), 389–412.
- Hanihara, T. (2000). Frontal and facial flatness of major human populations. *American Journal of Physical Anthropology*, 111(1), 105–134.
- Harvati, K., & Weaver, T. D. (2006). Human cranial anatomy and the differential preservation of population history and climate signatures. *The Anatomical Record. Part A, Discoveries in Molecular, Cellular, and Evolutionary Biology*, 288(12), 1225–1233.
- Hawkes, E. W. (1916). Skeletal measurements and observations on the point Barrow Eskimos with comparisons from other Eskimo groups. *American Anthropologist*, 18, 203–234.
- Hellman, M. (1927). Changes in the human face brought about by development. *International Journal of Orthodontia, Oral Surgery and Radiography*, 13(6), 475–516.
- Hennessy, R. J., & Stringer, C. B. (2002). Geometric morphometric study of the regional variation of modern human craniofacial form. *American Journal of Physical Anthropology*, 117(1), 37–48.
- Holton, N. E., & Franciscus, R. G. (2008). The paradox of a wide nasal aperture in cold-adapted Neandertals: A causal assessment. *Journal of Human Evolution*, 55(6), 942–951.
- Howells, W. (1973). *Cranial variation in man: A study by multivariate analysis of patterns of difference among recent human populations*. Cambridge: MA: Harvard University Press.
- Howells, W. (1989). *Skull shapes and the map: Craniometric analyses in the dispersion of modern homo*. Cambridge: MA: Harvard University Press.
- Hrdlička, A. (1910). Contributions to the anthropology of central and Smith sound Eskimo. *Anthropological Papers of the American Museum of Natural History*, 5, 177–280.
- Hubbe, M., Hanihara, T., & Harvati, K. (2009). Climate Signatures in the Morphological Differentiation of Worldwide Modern Human Populations. 292(11), 1720–1733.
- Hylander, W. L. (1977). The adaptive significance of Eskimo craniofacial morphology. In A. A. G. Dahlberg & M. Thomas (Eds.), *Orofacial growth and development* (pp. 129–169). The Hague: De Gruyter.
- Israel, H. (1968). Continuing growth in the human cranial skeleton. *Archives of Oral Biology*, 13(1), 133–141.
- Israel, H. (1977). The dichotomous pattern of craniofacial expansion during aging. 47(1), 47–51.
- Josse, J., & Husson, F. (2016). missMDA: A package for handling missing values in multivariate data analysis. *Journal of Statistical Software*, 70, 1–31.
- Kurihara, S., Enlow, D. H., & Rangel, R. D. (1980). Remodeling reversals in anterior parts of the human mandible and maxilla. *The Angle Orthodontics*, 50(2), 98–106.
- Le Minor, J.-M., Billmann, F., Sick, H., Vetter, J.-M., & Ludes, B. (2009). *Anatomies et Pathologies, les collections morphologiques de la Faculte de medecine de Strasbourg*: I.D. l'Édition.
- Lieberman, D. E., McBratney, B. M., & Krovitz, G. (2002). The evolution and development of cranial form in *Homo sapiens*. *Proceedings of the National Academy of Sciences*, 99(3), 1134–1139.
- Lynch, J. M., Wood, C. G., & Luboga, S. A. (1996). Geometric Morphometrics in primatology: Craniofacial variation in *Homo sapiens* and *Pan troglodytes*. *Folia Primatologica*, 67(1), 15–39.
- Lynnerup, N., Homøe, P., & Skovgaard, L. T. (1999). The frontal sinus in ancient and modern Greenlandic Inuit. *International Journal of Anthropology*, 14(1), 47–54.
- Maddux, S.D., Butaric, L.N., Yokley, T.R., & Franciscus, R.G. (2017). Ecogeographic variation across morphofunctional units of the human nose. 162(1), 103–119.
- Maddux, S. D., Yokley, T. R., Svoma, B. M., & Franciscus, R. G. (2016). Absolute humidity and the human nose: A reanalysis of climate zones and their influence on nasal form and function. *American Journal of Physical Anthropology*, 161(2), 309–320.
- Martinez-Maza, C., Freidline, S. E., Strauss, A., & Nieto-Diaz, M. (2015). Bone growth dynamics of the facial skeleton and mandible in Gorilla gorilla and *Pan troglodytes*. *Evolutionary Biology*, 43(1), 60–80.
- Martinez-Maza, C., Rosas, A., & Nieto-Diaz, M. (2013). Postnatal changes in the growth dynamics of the human face revealed from bone modeling patterns. *Journal of Anatomy*, 223(3), 228–241.
- Mayer, C., Metscher, B. D., Müller, G. B., & Mitteroecker, P. (2014). Studying developmental variation with geometric morphometric image analysis (GMIA). *PLoS One*, 9(12), e115076.
- McCollum, M. A. (1999). The robust australopithecine face: A morphogenetic perspective. *Science*, 284(5412), 301–305.
- McCollum, M. A. (2008). Nasomaxillary remodeling and facial form in robust Australopithecus: A reassessment. *Journal of Human Evolution*, 54(1), 2–14.
- Mitteroecker, P., Bartsch, S., Erking, C., Grunstra, N. D., Le Maître, A., & Bookstein, F. L. (2020). Morphometric variation at different spatial scales: Coordination and compensation in the emergence of organismal form. *Systematic Biology*, 69(5), 913–926.
- Mitteroecker, P., & Gunz, P. (2009). Advances in geometric morphometrics. *Evolutionary Biology*, 36(2), 235–247.
- Mitteroecker, P., Gunz, P., Windhager, S., & Schaefer, K. (2013). A brief review of shape, form, and allometry in geometric morphometrics, with applications to human facial morphology. *Biological Theory*, 24(1), 59–66.
- Mooney, M. P., & Siegel, M. I. (1986). Developmental relationship between premaxillary-maxillary suture patency and anterior nasal spine morphology. *The Cleft Palate Journal*, 23(2), 101–107.
- Morimoto, N., Ogihara, N., Katayama, K., & Shiota, K. (2008). Three-dimensional ontogenetic shape changes in the human cranium during the fetal period. *Journal of Anatomy*, 212(5), 627–635.
- Neubauer, S., Gunz, P., & Hublin, J.-J. (2010). Endocranial shape changes during growth in chimpanzees and humans: A morphometric analysis of unique and shared aspects. *Journal of Human Evolution*, 59(5), 555–566.

- Nicholas, C. L. (2016). Fetal and neonatal maxillary ontogeny in extant humans and the utility of prenatal maxillary morphology in predicting ancestral affiliation. *American Journal of Physical Anthropology*, 161(3), 448–455.
- Nicholson, E., & Harvati, K. (2006). Quantitative analysis of human mandibular shape using three-dimensional geometric morphometrics. 131(3), 368–383.
- Noback, M. L., & Harvati, K. (2015). The contribution of subsistence to global human cranial variation. *Journal of Human Evolution*, 80, 34–50.
- Noback, M.L., Harvati, K., & Spoor, F. (2011). Climate-related variation of the human nasal cavity. 145(4), 599–614.
- O'Higgins, P., Bromage, T. G., Johnson, D. R., Moore, W. J., & McPhie, P. (1991). A study of facial growth in the sooty Mangabey *Cercocebus atys*. *Folia Primatologica*, 56(2), 86–94.
- O'Higgins, P., & Jones, N. (1998). Facial growth in *Cercocebus torquatus*: An application of three-dimensional geometric morphometric techniques to the study of morphological variation. *Journal of Anatomy*, 193(2), 251–272.
- Oschinsky, L. (1962). Facial flatness and cheekbone morphology in arctic mongoloids: A case of morphological taxonomy. *Anthropological Papers of the American Museum of Natural History*, 4(2), 349–377.
- Ponce de Leon, M. S., & Zollikofer, C. P. E. (2001). Neanderthal cranial ontogeny and its implications for late hominid diversity. *Nature*, 412(6846), 534–538.
- Rampont, M. (1994). *Les squelettes, os et dents de foetus, nouveaux-nés et enfants du musée anatomique de Strasbourg. Aspects historiques et catalogues*. Strasbourg: Université Louis Pasteur.
- Rohlf, F. J., & Corti, M. (2000). Use of two-block partial least-squares to study Covariation in shape. *Systematic Biology*, 49(4), 740–753.
- Rohlf, F. J., & Slice, D. (1990). Extensions of the Procrustes method for the optimal superimposition of landmarks. *Systematic Zoology*, 39, 40.
- Rosas, A., & Bastir, M. (2002). Thin-plate spline analysis of allometry and sexual dimorphism in the human craniofacial complex. *American Journal of Physical Anthropology*, 117(3), 236–245.
- Roseman, C. C., & Weaver, T. D. (2004). Multivariate apportionment of global human craniometric diversity. *American Journal of Physical Anthropology*, 125(3), 257–263.
- RStudio Team. (2020). *RStudio: Integrated development environment for R*. Boston, MA: RStudio, PBC.
- Sardi, M. L., & Ramirez-Rozzi, F. V. (2012). Different cranial ontogeny in Europeans and southern Africans. *PLoS One*, 7(4), e35917.
- Schlager, S. (2017). Morpho and Rvcg—Shape analysis in R: R-packages for geometric Morphometrics, shape analysis and surface manipulations. In L. S. Z. Guoyan & S. Gabor (Eds.), *Statistical shape and deformation analysis* (pp. 217–256). London, England: Academic Press.
- Schlager, S., Profico, A., Di Vincenzo, F., & Manzi, G. (2018). Retrodeformation of fossil specimens based on 3D bilateral semi-landmarks: Implementation in the R package “Morpho”. *PLoS One*, 13(3), e0194073.
- Schneider, C. A., Rasband, W. S., & Eliceiri, K. W. (2012). NIH image to ImageJ: 25 years of image analysis. *Nature Methods*, 9(7), 671–675.
- Schuh, A., Kupczik, K., Gunz, P., Hublin, J.-J., & Freidline, S. E. (2019). Ontogeny of the human maxilla: A study of intra-population variability combining surface bone histology and geometric morphometrics. *Journal of Anatomy*, 235, 233–245.
- Schulte, F. A., Zwahlen, A., Lambers, F. M., Kuhn, G., Ruffoni, D., Betts, D., ... Müller, R. (2013). Strain-adaptive in silico modeling of bone adaptation — A computer simulation validated by in vivo micro-computed tomography data. *Bone*, 52(1), 485–492.
- Scott, N., Neubauer, S., Hublin, J.-J., & Gunz, P. (2014). A shared pattern of postnatal Endocranial development in extant hominoids. *Evolutionary Biology*, 41(4), 572–594.
- Smith, H. F. (2009). Which cranial regions reflect molecular distances reliably in humans? Evidence from three-dimensional morphology. *American Journal of Human Biology*, 21(1), 36–47.
- Stansfield, E., Evteev, A., & O'Higgins, P. (2018). Can diet be inferred from the biomechanical response to simulated biting in modern and pre-historic human mandibles? *Journal of Archaeological Science: Reports*, 22, 433–443.
- Stynder, D. D., Ackermann, R. R., & Sealy, J. C. (2007). Craniofacial variation and population continuity during the South African Holocene. *American Journal of Physical Anthropology*, 134(4), 489–500.
- Toro-Ibacache, V., Zapata Muñoz, V., & O'Higgins, P. (2016). The relationship between skull morphology, masticatory muscle force and cranial skeletal deformation during biting. *Annals of Anatomy - Anatomischer Anzeiger*, 203, 59–68.
- Viðarsdóttir, S., & O'Higgins, P. (2003). Developmental variation in the facial skeleton of anatomically modern *Homo sapiens*. In K. G. Thompson & A. Nelson (Eds.), *Patterns of growth and development in the genus homo* (pp. 114–143). Cambridge: Cambridge University Press.
- Viðarsdóttir, U. E., O'Higgins, P., & Stringer, C. (2002). A geometric morphometric study of regional differences in the ontogeny of the modern human facial skeleton. *Journal of Anatomy*, 201, 211–229.
- von Cramon-Taubadel, N. (2011). Global human mandibular variation reflects differences in agricultural and hunter-gatherer subsistence strategies. *Proceedings of the National Academy of Sciences*, 108(49), 19546–19551.
- von Cramon-Taubadel, N. (2014). Evolutionary insights into global patterns of human cranial diversity: Population history, climatic and dietary effects. *Journal of Anthropological Sciences*, 92, 43–77.
- Waddington, C. H. (1942). Canalization of the development and the inheritance of acquired characters. *Nature*, 150, 563–565.
- Williams, S. E., & Slice, D. E. (2010). Regional shape change in adult facial bone curvature with age. *American Journal of Physical Anthropology*, 143(3), 437–447.
- Windhager, S., Mitteroecker, P., Rupiç, I., Lauc, T., Polašek, O., & Schaefer, K. (2019). Facial aging trajectories: A common shape pattern in male and female faces is disrupted after menopause. *American Journal of Physical Anthropology*, 169(4), 678–688.
- Wolpoff, M. (1968). Climatic influence on the skeletal nasal aperture. *AJPA*, 29, 405–424.
- Yokley, T. R. (2009). Ecogeographic variation in human nasal passages. *American Journal of Physical Anthropology*, 138(1), 11–22.

## SUPPORTING INFORMATION

Additional supporting information may be found online in the Supporting Information section at the end of this article.

**How to cite this article:** Schuh A, Gunz P, Villa C, Kupczik K, Hublin J-J, Freidline SE. Intraspecific variability in human maxillary bone modeling patterns during ontogeny. *Am J Phys Anthropol*. 2020;1–16. <https://doi.org/10.1002/ajpa.24153>